European Journal of Pharmaceutical Sciences 103 (2017) 36–46

Contents lists available at ScienceDirect

European Journal of Pharmaceutical Sciences

journal homepage: www.elsevier.com/locate/ejps

A new construct of antibody-drug conjugates for treatment of B-cell non-Hodgkin's lymphomas

Libin Zhang [a,1], Yixin Fang [a,1], Jindřich Kopeček [a,b,*], Jiyuan Yang [a,**]

[a] Department of Pharmaceutics and Pharmaceutical Chemistry/CCCD, University of Utah, Salt Lake City, UT 84112, USA
[b] Department of Bioengineering, University of Utah, Salt Lake City, UT 84112, USA

ARTICLE INFO

Article history:
Received 5 January 2017
Received in revised form 24 February 2017
Accepted 24 February 2017
Available online 27 February 2017

Keywords:
N-(2-hydroxypropyl)methacrylamide (HPMA)
Antibody-drug conjugates (ADCs)
Rituximab
B cell lymphoma
Epirubicin

ABSTRACT

The aim of this study was to develop a new class of antibody-drug conjugates (ADCs) with the potential to not only enhance treatment efficacy but also improve tolerability for patients with B-cell lymphomas. Classic ADCs consist of monoclonal antibodies (mAbs) linked to drugs or toxins. They selectively deliver toxic moieties to tumor cells. As such, they greatly improve the therapeutic index compared to traditional chemotherapeutic agents. However, the therapeutic efficacy and safety of ADCs are dependent on linker stability and payload toxicity. Limited payload number on a single antibody (drug-to-antibody ratio, or DAR) has been driving investigators to use extremely toxic agents; however, even very low off-target binding of these ADCs may kill patients. Herein we report a new design of ADCs that consists of rituximab (RTX) and *N*-(2-hydroxypropyl)methacrylamide (HPMA) copolymer–epirubicin conjugates. The latter was selectively attached to RTX via reduced disulfide bonds. Such design allows the introduction of a large payload of drug on the antibody without adding attachment sites and without compromising the antigen-targeting ability. The binding of the new conjugate, namely RTX-P-EPI, to Ramos cells (with high CD20 expression) was confirmed. The cytotoxicity of RTX-P-EPI against Raji and Ramos cells was also determined. Interestingly, two-fold inhibition of cell proliferation was observed when using RTX-P-EPI compared with their equivalent physical mixture of RTX and P-EPI. Treatment of male SCID mice bearing subcutaneous Ramos B-cell lymphoma tumors demonstrated that RTX-P-EPI possessed superior efficacy when compared to combination of RTX with chemotherapy EPI (RTX + EPI) and P-EPI (RTX + P-EPI), whereas single RTX and a non-specific conjugate IgG-P-EPI only showed marginal effect. The conjugate RTX-EPI in which EPI was directly attached to RTX demonstrated much less antitumor activity compared with RTX-P-EPI. The results suggest that this new design possesses synergistic potential of immunotherapy combined with established macromolecular therapy; moreover, a conventional chemo-agent could be utilized to generate highly effective ADCs and to achieve lower risk of off-target toxicity.

1. Introduction

Non-Hodgkin lymphoma (NHL), a frequent hematologic malignancy, is the 6th most common cancer and the 9th leading cause of cancer death in the United States (Siegel et al., 2016). Treatment of NHL is challenging because the disease comprises over 35 different subtypes with the most prevalent types being diffuse large B cell lymphoma, follicular lymphoma and mantle cell lymphoma (Chu and Polson, 2013). Eighty-five percent of NHLs are of B-cell origin, and >95% of B-cell lymphomas bear the cell surface antigen CD20 (Cheson and Leonard, 2008). The discovery of rituximab, the first FDA approved monoclonal antibody against CD20, initiated a new era for treatment of B-cell NHLs (Leget and Czuczman, 1998). Its combination with chemotherapy can further enhance the therapeutic activity and still serves as clinical golden standard (Zelenetz et al., 2014). With the development of new, more active modern chemotherapy protocols and targeted therapies, much progress has been made over the past two decades (Alley et al., 2010; Mehta and Forero-Torres, 2015; Richter et al., 2016; Seyfizadeh et al., 2016). Unfortunately, besides adverse side effects, relapsed or resistant disease remains a major cause of treatment failure. The nonresponsiveness and/or resistance have been attributed to the inability of immune effector cells to hypercrosslink ligated mAbs, and Fc receptor-mediated endocytosis or "trogocytosis" of CD20 antigens (Chu and Kopeček, 2015). Thus, the need for new therapeutic strategies that combine high levels of efficacy with improved tolerability is evident.

An ideal strategy would be the development of highly 'specific' drugs that only accumulate in and kill tumor cells to achieve tumor

* Correspondence to: J. Kopeček, Center for Controlled Chemical Delivery (CCCD), 20 S 2030 E, BPRB 205B, University of Utah, Salt Lake City, UT 84112-9452, USA.
** Correspondence to: J. Yang, Center for Controlled Chemical Delivery (CCCD), 20 S 2030 E, BPRB 205C, University of Utah, Salt Lake City, UT 84112-9452, USA.
E-mail addresses: jindrich.kopecek@utah.edu (J. Kopeček), jiyuan.yang@utah.edu (J. Yang).
[1] Equal contribution.

http://dx.doi.org/10.1016/j.ejps.2017.02.034
0928-0987/

eradication without systemic toxicity. Antibody-drug conjugates (ADCs) are such an approach that allows for targeted delivery of cytotoxic agents to antigen-expressing tumor cells (Chari et al., 2014; Jagadeesh and Smith, 2016). ADCs consist of three components: the antibody (Ab), linker and drug/toxin (Ducry and Stump, 2010). The concept of using Ab for drug delivery is not new, however, the design of an ADC remains challenging, as it involves multiple factors, for example, selection of an antibody, the stability of a linker, the payload and its cleavage kinetics, etc. Among them a critical parameter is payload number on a single antibody (drug-antibody ratio or DAR), because over-attachment will disturb mAb immunoaffinity. Generally, only a limited number of toxin moieties can be attached to one Ab molecule (usually DAR is 4–6). Consequently, extremely toxic agents such as calicheamicin or auristatin monomethyl ester (MMAE) with $IC_{50} < 1$ nM have to be employed in order to obtain sufficient efficacy for target cell death (Casi and Neri, 2012; Wu and Senter, 2005). Therefore, even a little fraction off-target conjugate will result in serious adverse effects.

Development of ADCs for B-cell NHL is rational, because NHL has been treated clinically with either chemotherapy or immunotherapy (i.e. RTX), or their combination; it is anticipated that the tumor cells will be responsive to cytotoxic agents delivered by an ADC. Given the fact that RTX has been used in clinical practice for over two decades, the antibody and the target have been extensively validated. Moreover, the efficacy of RTX has been increased when used in combination with chemotherapy, thus RTX-based ADCs may provide potential synergism.

However, it has been reported that directly conjugated conventional chemotherapy drugs such as doxorubicin (DOX) to an Ab have failed due to lack of cytotoxic potency (Braslawsky et al., 1991; Tolcher et al., 1999). HPMA copolymer-DOX conjugates were attached to RTX but did not enhance treatment activity in vivo when compared to controls (Lidický et al., 2015). Herein we demonstrate an innovative way to generate therapeutically efficient ADCs by using semitelechelic HPMA copolymer-epirubicin conjugates attached to RTX, resulting in multiple drugs bound to an Ab to enhance overall cytotoxicity and treatment efficacy of an ADC but without adding attachment sites. The antigen-targeting ability and pharmacokinetics of the ADC, namely RTX-P-EPI, are preserved. This new generation of conjugates possesses the unique features of both antibody-drug conjugates with high specificity and advantages of macromolecular therapeutics. To examine the potent therapeutic activity of the new ADCs, in vitro and in vivo assays have been used. The binding affinity of RTX to Ramos cells before and after conjugation was analyzed using flow cytometry. The antitumor efficacy of the new ADC - RTX-P-EPI was evaluated on male NOD SCID mice bearing subcutaneous Ramos B-cell lymphoma tumors.

2. Materials and methods

2.1. Materials

2.1.1. Chemicals

All solvents were purchased with the highest grade from Fisher Scientific (Pittsburgh, PA) and used as received. Dicyclohexylcarbodiimide (DCC), 4-(dimethylamino)pyridine (DMAP), and HATU(1-[bis(dimethylamino)methylene]-1H-1,2,3-triazolo[4,5-*b*]pyridinium 3-oxid hexafluoro-phosphate) were purchased from AAPPTEC (Louisville, KY). Iodine-125 [^{125}I] was from Perkin-Elmer. Bicinchoninic acid (BCA) protein assay kit and tris(2-carboxyethyl)phosphine (TCEP) were from Thermo Scientific Pierce (Rockford, IL). Thiazolidine-2-thione (TT), *N*-2-aminoethylmaleimide trifluoroacetate and diisopropylethylamine (DIPEA) were purchased from Sigma-Aldrich (St. Louis, MO). Cy5-NHS ester was from Lumiprobe (Hallandale Beach, FL). 2,2′-Azobis(2,4-dimethylvaleronitrile) (V65), 2,2′-azobis(4-methoxy-2,4-dimethylvaleronitrile) (V70) were from Wako USA (Richmond, VA). Epirubicin hydrochloride was purchased from DKY Technology (Wuhan, China). *N*-(2-hydroxypropyl)methacrylamide (HPMA) (Kopeček and Bažilová, 1973), *N*-methacryloylglycylphenylalanylleucylglycine (MA-GFLG-OH) (Ulbrich et al., 2000), *N*-methacryloylglycylphenylalanylleucylglycine-epirubicin (MA-GFLG-EPI) (Yang et al., 2015), and 4-cyanopentanoic acid dithiobenzoate (CPDB) (Mitsukami et al., 2001) were synthesized according to literatures.

2.1.2. Cells and reagents

Ramos and Raji Burkitt's lymphoma cell lines were from American Type Culture Collection (ATCC) (Manassas, VA) and maintained at 37 °C in a humidified atmosphere containing 5% CO_2 in RPMI-1640 medium (Gibco) supplemented with 10% FBS and a mixture of antibiotics (100 units/ml penicillin, 0.1 mg/ml streptomycin). Rituximab (Genentech) was obtained from Hunstman Cancer Hospital, University of Utah at a stock concentration of 10 mg/ml. Human IgG was from Sigma (St. Louis, MO). Alexa Fluor® 488 goat anti-human IgG (H + L) was from Thermo Fisher Scientific (Waltham, MA). Cell Counting Kit-8 (CCK-8) was from Dojindo (Rockville, MD). Annexin V-FITC Apoptosis Kit was purchased from Clontech (Mountain View, CA).

2.1.3. Animals

About 7–9 weeks old male NOD SCID mice (25–30 g) were bred in-house (originally purchased from Jackson Laboratories (Bar Harbor, ME)). Animals were housed in the Animal Facility of the Comparative Medicine Center at the University of Utah under standard conditions. Procedures involving animals and their care were conducted following approved Institutional Animal Care and Use Committee (IACUC) protocols.

2.2. Synthesis of antibody-drug conjugates

2.2.1. Synthesis of 2-cyano-5-oxo-5-(2-thioxothiazolidin-3-yl)pental-2-yl benzodithioate (CTA-TT)

CTA-TT was synthesized as previously described (Tao et al., 2009). In brief, 0.84 g CPDB, 0.36 g TT and 0.025 g DMAP were dissolved in 10 ml dichloromethane (DCM) and precooled with ice bath. DCC in 10 ml DCM was added dropwise to the flask within 30 min, then stirring continued for 6 h in dark at room temperature (r.t.). After working up, filtration (to remove precipitated salts) gave rise to a red filtrate. The solution was concentrated by rotary-evaporator. CTA-TT is purified via silica gel column chromatography (70–230 mesh, 60 Å) using gradient ethylacetate/hexane (step gradient 1:3 to 1:1, v/v) as eluent. The fraction was evaporated under reduced pressure. The CTA-TT agent was obtained as red oil. ^{1}H NMR $CDCl_3$ (ppm): 7.60–7.30 (benzene), 4.60–4.50 (NCH_2CH_2), 3.40–3.20 (SCH_2CH_2), 2.70–2.60 (CCH_2CH_2), 2.60–2.50 (CCH_2CH_2), 2.20–2.10 (CCH_2CH_2), 2.00–1.90 (CH_3).

2.2.2. Synthesis of semitelechelic maleimide functionalized HPMA copolymer-epirubicin conjugate (ST-P-EPI-Mal)

Semitelechelic (ST) HPMA copolymers terminated with maleimide group were prepared by RAFT copolymerization followed by two-step end modification. A typical polymerization process is briefly summarized as follows: an ampoule containing HPMA (139 mg, 0.97 mmol) and MA-GFLG-EPI (30 mg, 0.03 mmol) were attached to the Schlenk-line. After three vacuum-nitrogen cycles to remove oxygen, CTA-TT (4 mg/ml × 170 μl, in degassed MeOH/H^+ 0.3% acetic acid) and V70 (1 mg/ml × 184 μl, in degassed MeOH/H^+ 0.3% acetic acid) were added via syringe under magnetic stirring and bubbled with N_2 for 10 min in ice bath. The ampoule was sealed, and polymerization was performed at 30 °C for 22 h. The copolymer was obtained by precipitation into acetone/ethyl ether and purified by redissolving in methanol and precipitation in acetone/ethyl ether two more times. The copolymer was isolated as red powder and dried under vacuum. The average molecular weight (*Mw*) and the polydispersity (*PDI*) of the conjugates were determined using size-exclusion chromatography (SEC) on an ÄKTA FPLC system equipped with a UV detector (GE Healthcare), mini

DAWN TREOS, and OptilabrEX (refractive index) detector (Wyatt Technology) using a Superose 6 HR10/30 column with sodium acetate buffer containing 30% acetonitrile (pH 6.5) as mobile phase. The dithiobenzoate group was removed by further reaction with 40-times excess V-65 in 0.3 ml MeOH/H^+ at 55 °C for 2 h, and precipitation into acetone/ethyl ether twice, resulting in *ST*-P-EPI-TT (70 mg, 41%). The content of EPI in copolymer was determined spectrophotometrically (λ_{max} = 495 nm) by dissolving *ST*-P-EPI-TT in methanol (~2 mg/10 ml) and calculated according to EPI standard curve in methanol.

The end-chain reactive maleimide (mal) group was incorporated by the reaction of TT group with *N*-(2-aminoethyl)maleimide. For example, 18 mg *ST*-P-EPI-TT was dissolved in 500 μl DMSO, then the solution was added into 0.1 ml DMSO containing 10 μl DIPEA and 5 mg *N*-(2-aminoethyl)maleimide trifluoroacetate. After stirring at r.t. for 24 h, the polymer was isolated by precipitation in acetone/ether three times to yield 16.5 mg *ST*-P-EPI-mal. The presence of maleimide group was confirmed by modified Ellman assay.

2.2.3. Synthesis of antibody-polymer-EPI conjugates

13 mg rituximab was buffer changed with Tris-HCl buffer (20 mM, 5 mM EDTA, pH 7.4) to final volume 2.5 ml and mixed with TCEP (100 mM × 300 μl, 80 times excess in Tris-HCl buffer, pH 7.4). After incubation at 37 °C for 3 h, the excess TCEP was removed by ultrafiltration (EMD Millipore Amicon™, MWCO 30,000) four times with Tris buffer to yield RTX-SH. *ST*-P-EPI-Mal (16.5 mg, in 400 μl Tris·HCl buffer) was added into RTX-SH solution, and incubated at 37 °C for 6 h. After working up, the conjugate was purified using SEC on ÄKTA FPLC system (GE Healthcare, Piscataway, NJ) equipped with Sephacryl S-100 HR16/60 column eluted with PBS (pH 7.2) to remove free, unconjugated *ST*-P-EPI.

Following the same procedure, non-specific IgG-P-EPI was prepared. The protein concentration (RTX or IgG) in final solution was determined with BCA protein assay, whereas the polymer content was evaluated using UV–vis spectroscopy based on EPI content. Consequently, the substitution degree (P-EPI/mAb) and drug-to-antibody ratio (DAR) were calculated.

2.2.4. Synthesis of RTX-EPI conjugate

To synthesize maleimide modified epirubicin, 6-(2,5-dioxo-2,5-dihydro-1H-pyrrol-1-yl)hexanoic acid (12 mg, 0.06 mmol) was dissolved in 200 μl DMF, HATU (0.05 mmol) and DIPEA (20 μl) was added and stirred at r.t. for 30 min. The mixture was transferred into EPI (27 mg, 0.05 mmol) solution with 15 μl DIPEA in 100 μl DMF. The reaction mixture was stirred at r.t. overnight to yield EPI-mal. The product was purified by HPLC (Agilent ZORBAX, 5 μm, 300SB-C18 column 9.4 × 250 mm, using flow rate 2.5 ml/min and gradient elution from 2% to 90% of buffer B within 30 min. Buffer A: DI H_2O, buffer B: acetonitrile). The structure and purity of the product were confirmed by MALDI-TOF-MS and HPLC analysis. MS (MALDI-TOF) *m/z*: 759.21 $[M + Na]^+$, 775.18 $[M + K]^+$.

RTX-SH was prepared as described above. EPI-mal (10 mM × 35 μl in DMSO) was added into RTX-SH solution, and incubated at r.t. for 2 h and purified by ultrafiltration (30,000 Da cut-off) four times with PBS. The molar ratio of EPI/RTX was calculated by UV–vis absorbance as 3.1.

2.2.5. RTX labeled with Cy5

Rituximab (10 mg/ml × 300 μl) in PBS was buffer changed with added PBS buffer (pH 8.0) three times. Cy5-NHS (5 mg/ml × 8 μl, in DMSO, RTX: Cy5 = 1:3) was added and incubated at r.t. for 2 h to yield RTX-Cy5. The free Cy5-NHS was removed by PD-10 column and ultrafiltration (30,000 Da cut-off) three times. The RTX concentration in the final RTX-Cy5 solution was determined by BCA assay, and the Cy5 content was determined by UV–visible spectroscopy (molar extinction coefficient: 125,000 M^{-1} cm^{-1} at 645 nm in PBS). The ratio of Cy5/RTX was 0.8.

2.3. Sodium dodecyl sulfate polyacrylamide gel electrophoresis (SDS-PAGE)

Samples were prepared in SDS-PAGE loading buffer. The samples were loaded onto (6–10%) acrylamide gel run at 110 V and 30 mA for 1.5 h in 1 × running buffer (25 mM Tris·HCl, 250 mM glycine, and 0.1% SDS) on a Bio-Rad Mini-PROTEAN gel apparatus.

2.4. Binding affinity evaluation

To evaluate cell binding of antibody and antibody-polymer-drug conjugate, Ramos cell line with high CD20 expression was selected as target. Cells (2×10^5 in 400 μl medium) were centrifuged by 2000 RPM for 5 min, the supernatant was removed and the final volume was about 50 μl. Conjugates with increasing concentration (0.04, 0.2 or 1 μg in 20 μl PBS) were added. IgG-P-EPI and RTX were used for comparison. Cells were incubated at 4 °C for 20 min and washed with medium twice to remove unbound conjugates. Cells were then stained with 100 μl secondary antibody (Alexa Fluor® 488 goat-anti human IgG (H + L), 1:200 diluted) and incubated at 4 °C for another 20 min. After washing by PBS twice, labeled cells were analyzed by flow cytometry.

2.5. In vitro cell growth inhibition and apoptosis

2.5.1. Cell growth inhibition

The cytotoxicity of antibody and antibody-polymer-drug conjugates against Ramos cells was measured by CCK-8 assay (Dojindo). The cells were seeded in 96-well plates at the density of 10,000 cells (200 μl) per well in RMPI-1640 medium containing 10% FBS. After 24 h, RTX, RTX-EPI RTX-P-EPI, mixture of RTX with P-EPI and IgG-P-EPI (0.3 mg/ml × 15 μl for antibody) in medium was added and incubated at 37 °C for 48 h. The number of viable cells was estimated using CCK-8 kit according to the manufacturer's protocol. In brief, 50 μl 5× diluted CCK-8 solution was added and incubated at 37 °C, 5% CO_2 for 4 h, the absorbance was measured using a microplate reader at 450 nm (630 nm as reference). Untreated control cells were set as 100% viable.

2.5.2. Apoptosis

Annexin V-FITC and PI staining were performed following the RAPID ™ protocol provided by the manufacturer. 2×10^5 Ramos cells were suspended in 0.4 ml fresh growth medium containing 0.2 μM (antibody) RTX, RTX-EPI, RTX-P-EPI, IgG-P-EPI or mixture of RTX and P-EPI (the concentration of P-EPI was equal to the content of RTX-P-EPI). The cell suspension was incubated for 48 h. For Raji cells, various treatments were applied and cells were incubated for 24 h. All experiments were carried out in triplicate.

2.6. Internalization

2.6.1. Confocal fluorescence microscopy

Ramos cells at a density of 2×10^5 in 100 μl medium were incubated with RTX-Cy5 or RTX-P-EPI (3 mg/ml × 25 μl) in culture medium at 37 °C for 3 h; then the cells were washed twice with PBS to remove unbound conjugates and plated onto sterile 35-mm glass bottom dishes with 14-mm microwells (MatTek Corporation, Ashland, MA) for imaging, using Olympus laser scanning confocal microscope (FV 1000).

2.6.2. Flow cytometry

10^6 Ramos cells in 100 μl culture medium were mixed with RTX-P-EPI (6 mg/ml × 5 μl) and incubated at 4 °C for 30 min. Unbound conjugates were removed by washing cells in medium to final volume 500 μl. Cells were incubated at either at 37 °C in medium or 4 °C with NaN_3 (0.1%). At indicated time points, 100 μl of cells was removed from culture, then stained with 100 μl secondary antibody (Alexa Fluor® 488 goat-anti human IgG (H + L), 1:200 diluted) and incubated at 4 °C for

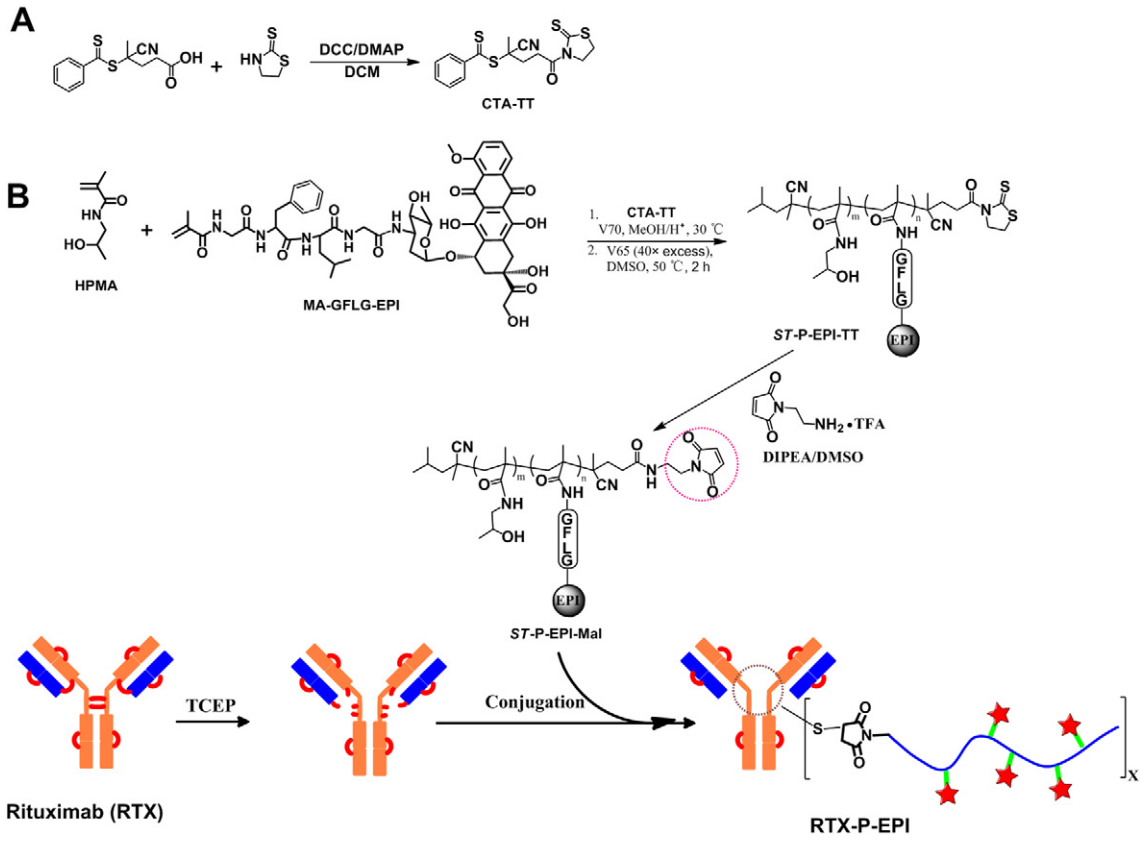

Scheme 1. Synthesis of semitelechelic maleimide-functionalized HPMA copolymer-epirubicin conjugate (*ST*-P-EPI-Mal) and its attachment to rituximab via reduced thiol group.

another 20 min. After washing twice with PBS, labeled cells were analyzed by flow cytometry.

2.7. In vivo evaluation of antitumor efficacy

Localized xenograft model of human B-lymphoma was used to evaluate the efficacy of RTX-P-EPI. Ramos cells (5×10^6) in 200 μl of PBS were subcutaneously inoculated in theright flank of mice. Tumor size was measured with a caliper, and tumor volume was calculated according to the formula: tumor volume (mm^3) = 1/2 × length × $(width)^2$, where the length (mm) is the longest and the width (mm) is the shortest dimension of the tumor. When the average tumor size reached 150 ± 50 mm^3, treatment was initiated (n = 4–5). Mice were intravenously (i.v.) administered via tail vein (on days 11, 14, 17, and 20 after tumor implantation) with RTX-P-EPI and a series of references including unconjugated RTX, non-specific IgG-P-EPI, free EPI directly conjugated RTX-EPI, and combination of RTX with EPI or P-EPI. Body weight variation was computed by the equation: variation = $(W_{Dayn} - W_{Day0}) / W_{Day0} \times 100\%$.

2.8. Pharmacokinetics and biodistribution

The conjugates were radioiodinated by the Iodogen method as previously described (Liu et al., 2009). 7–9 weeks old healthy male NOD SCID mice (n = 3) were intravenously injected with ^{125}I labeled RTX, RTX-P-EPI or IgG-P-EPI conjugates (0.1 mg, 20 μCi per mouse), respectively. At predetermined intervals, blood samples (10 μl) were taken from the tail vein, and the radioactivity of each sample was measured with Gamma Counter (Packard).

For biodistribution study, 7–9 week-old male NOD SCID mice bearing *s.c.* Ramos tumors received intravenous injection of ^{125}I labeled RTX, RTX-P-EPI, or IgG-P-EPI (0.1 mg, 20 μCi per mouse). At 72 and 96 h after administration, the mice were sacrificed. Various tissues (heart, liver, spleen, lung, kidney, stomach, intestine, muscle, bone, brain and tumor) were harvested, weighed, and counted for radioactivity with Gamma Counter (Packard). Uptake of the conjugate was calculated as the percentage of the injected dose per gram of tissue (% ID/g). Data are presented as mean ± standard deviation (n = 3).

2.9. Statistics

All experiments in this study were at least triplicated. Quantitative analyses are presented as mean ± standard deviation (SD). One-way analysis of variance (ANOVA) coupled with Tukey's post hoc analysis was used to compare three or more groups (with p value <0.05 indicating statistically significant difference).

3. Results

3.1. Design, preparation and characterization of antibody-drug conjugate RTX-P-EPI

Conjugation of drugs to an antibody usually takes place at a solvent accessible lysine or cysteine. A human IgG comprises about 100 lysine residues. About half of them, located at both heavy chains and light chains, are accessible and could be modified, resulting in a heterogeneous mixture of conjugates with DAR being 0 to 8. This implicates that wide range of in vivo pharmacokinetic properties will be generated with this unspecific approach. Cysteine conjugation occurs after

Table 1
Characterization of *ST*-P-EPI.

Polymer precursor	*Mn* (kDa)	*Mw*/*Mn*	EPI wt%	EPI/polymer chain
ST-P-EPI-1	37.9	1.17	9.4	6.6
ST-P-EPI-2	32.9	1.11	8.0	4.7

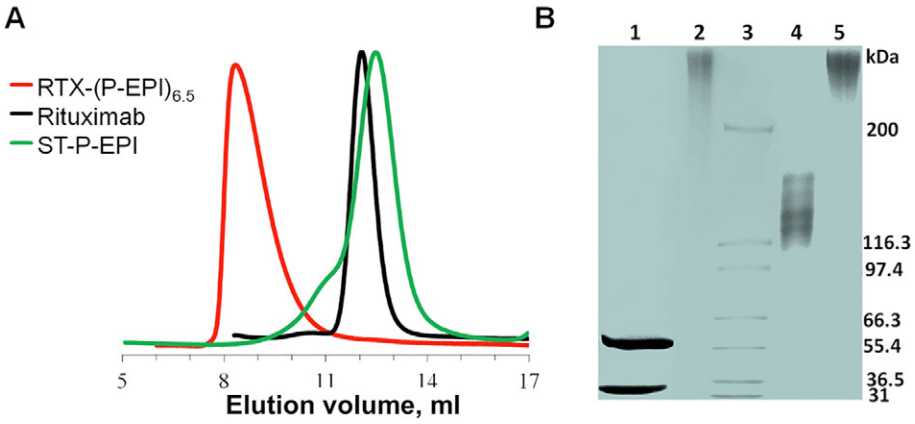

Fig. 1. (A) SEC analysis of ST-P-EPI, RTX and RTX-(P-EPI)$_{6.5}$; (B) SDS-PAGE analysis of conjugates staining with Coomassie blue. Lane 1: RTX-EPI (DTT+); Lane 2: IgG-P-EPI; Lane 3: marker; Lane 4: IgG; Lane 5: RTX-P-EPI.

reduction of four interchain disulfide bonds that yields ≤8 of exposed sulfhydryl groups. Consequently, the resulting ADCs have a lower degree of heterogeneity. Therefore, conjugation via cysteine residue was selected, and the designed synthetic approach is depicted in Scheme 1: Maleimide-modified semitelechelic HPMA copolymer-epirubicin conjugate was first prepared, then attached to RTX via thioether bonds as a result of thiol-ene reaction.

The copolymer precursor was prepared by RAFT copolymerization of HPMA with MA-GFLG-EPI. The use of chain transfer agent CTA-TT enables preparation of copolymers with a reactive TT group at one chain (macromolecule) end. To ensure the polymer carrier eventual elimination, the average molecular weight of a polymer precursor was controlled to be below the renal threshold (<~50 kDa). *ST*-P-EPI-TT contained 0.89 end TT groups at the end of polymer (determined by UV spectrophotometry using molar extinction coefficient of monomer 10,800 $L \cdot mol^{-1}\ cm^{-1}$ in MeOH at 305 nm, UV spectrophotometry of EPI at 305 nm as base line). ST-P-EPI-mal contained 0.86 maleimide groups per polymer, which was determined by modified Ellman's assay (Gergel and Cederbaum, 1996). EPI precursors were synthesized following the same procedure. Their characterization is summarized in Table 1.

To attach the active copolymer precursors to RTX, RTX was treated with TCEP in Tris·HCl buffer (pH 7.4). Under such mild condition, the solvent-accessible four inter-chain disulfide bonds were reduced into thiol groups (RTX-SH). Ellman assay (Gergel and Cederbaum, 1996) showed that the thiol/mAb ratio of RTX-SH was 7.9. SEC analysis showed the same elution volume with RTX, which is coincident with a previous report (Zhang et al., 2015) and indicated the same molecular weight with RTX. RTX-SH was reacted with excess of *ST*-P-EPI in Tris·HCl buffer. SEC analysis showed that after attachment, the peak corresponding to RTX completely disappeared, accompanied by a new peak corresponding to the conjugate RTX-P-EPI (Supporting information Fig. S1). The SEC profiles of pure RTX-P-EPI, RTX and polymer precursor *ST*-P-EPI are shown in Fig. 1A.

As control (for biological evaluation), non-specific human IgG-P-EPI and a conjugate RTX-EPI in which EPI was directly attached to RTX were also prepared (Scheme 2).

Sodium dodecyl sulfate polyacrylamide gel electrophoresis (SDS-PAGE) analysis further confirmed the successful synthesis of RTX-P-EPI: non-denatured product (Fig. 1B Lane 5) validated the disappearance of the free antibody band, accompanied by the emergence of smears with higher apparent molecular weights corresponding to the conjugate RTX-P-EPI.

To elucidate the relationship between substitution degree of *ST*-P-EPI and retained RTX binding ability, four RTX-P-EPI conjugates with various of DAR were prepared by changing the feed ratio of [*ST*-P-EPI-mal]/[RTX-SH] and reaction time. Their characterization is summarized in Table 2.

Unlike classic ADCs in which higher payload causes association and impairs solubility, in our system, even when the DAR reaches over 40 (No. 5 RTX-(P-EPI)$_{6.5}$), the conjugate was still water-soluble, and there was no aggregation detectable (Fig. 2).

3.2. Binding affinity of various conjugates to Ramos B-cells

To ensure CD-20 antigen expression on the surface of Ramos cells we used, Ramos cells were exposed to RTX labeled with Cy5 (RTX-Cy5). Flow cytometry analysis showed a high Cy5 signal of incubated Ramos cells. Nevertheless, if CD20 receptors were blocked with an over-saturation dose of RTX, there was no Cy5 signal detectable following

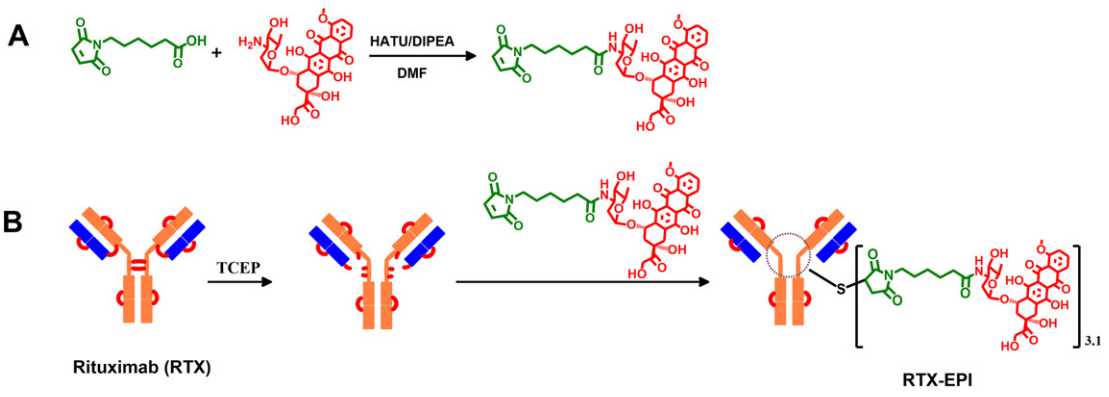

Scheme 2. Synthesis of maleimide-modified epirubicin (A) and attachment to rituximab via reduced thiol groups (B).

incubation of cells with RTX-Cy5 (Supporting information Fig. S2). This confirmed the expression of CD20 on the surface of the Ramos cells, and their specific binding affinity to RTX.

To evaluate the binding characteristics of antibody-drug conjugates, Ramos cells were treated with three different amounts of RTX or equivalent RTX-drug conjugates, incubated at 4 °C to block antigen modulation, and washed to remove unbound material. Goat antihuman IgG fluorescently labeled secondary antibody was used to determine mean fluorescence intensity (MFI) of each conjugate sample. Higher MFI indicates more bound conjugates.

Fig. 3 shows the binding affinity was influenced by the ratio of polymer to antibody in all three concentrations used. As expected, IgG-P-EPI barely bound to Ramos cells; modification of RTX with P-EPI partially decreased the binding affinity in a 'valency' dependent manner; the higher the attachment of polymer-precursor, the higher the decrease of conjugate binding. At given concentration (1 μg Ab), when 3 polymer chains were attached at the inter chain disulfide-binding sites of RTX, the conjugate (RTX-(P-EPI)$_{3.1}$) showed over 50% binding affinity retention compared with unconjugated RTX, whereas conjugates with 4.5 and 5.6 polymer chains (RTX-(P-EPI)$_{4.5}$, RTX-(P-EPI)$_{5.6}$) showed about 40% and 30% binding affinity retention, respectively. RTX-(P-EPI)$_{6.5}$ showed similar binding affinity with RTX-(P-EPI)$_{5.6}$. Therefore, for further in vitro cytotoxicity and in vivo efficacy evaluation, the conjugate RTX-(P-EPI)$_{3.1}$ was used, and simply denoted as RTX-P-EPI.

3.3. In vitro toxicity of antibody-polymer-drug conjugates

The cytotoxicity of RTX-P-EPI against Ramos cells was first evaluated at the concentration of 0.15 μM (related to RTX). Unconjugated RTX, non-specific conjugate IgG-P-EPI and directly conjugated with free drug (RTX-EPI) were used as controls. The Ramos cells were incubated with the samples for 48 h and evaluated by CCK-8 assay (Fig. 4). Under the given condition, all the new design conjugates RTX-(P-EPI)x (x = 3.1, 4.4, 5.6, 6.5) exhibited remarkable ability to inhibit proliferation of Ramos cells (about 40% kill) regardless of the variable substitution degrees, whereas the cytotoxicity of RTX alone was nearly undetectable. Especially, the advantage of antibody-polymer-drug conjugates was demonstrated in comparison with the classic antibody-drug conjugate RTX-EPI (18% kill) and the mixture of RTX and P-EPI (the equal concentration of RTX and EPI with RTX-(P-EPI)$_{3.1}$, 30% kill). Non-specific conjugate IgG-P-EPI (22% kill) showed moderate cytotoxicity. These results implicate the potential clinical application of RTX-P-EPI, an antibody conjugated with conventional chemotherapeutics.

To further investigate the antitumor activity of the new design conjugate RTX-P-EPI, Ramos and Raji cells were used to detect the apoptosis level induced by the conjugate. Cells (2×10^5/well) were incubated at concentration of 0.2 μM RTX equivalent for 48 h (for Ramos) or 24 h (for Raji). Apoptosis induction of cells was analyzed using Annexin V/PI staining. For control samples, IgG-P-EPI had minimal cytotoxicity, while RTX-EPI or RTX + P-EPI had similar cytotoxicity as RTX alone. By contrast, RTX-P-EPI had markedly increased cytotoxicity compared with all three RTX-containing groups (Fig. 5). The superiority of RTX-P-EPI was also observed in Raji cells. When cells were treated with RTX alone, increase of antibody concentration from 0.2 μM to 2 μM did not significantly enhance the apoptosis level, suggesting that antibody binding to the cells may have reached saturation. However, when cells were first treated with a high concentration of RTX (2 μM) followed 1 h later by exposure to 0.2 μM equivalent RTX-P-EPI, the percentage of apoptotic cells almost doubled, which indicates that RTX-P-EPI could be active against RTX-pretreated cells. This raises the likelihood that this system may be efficient in the treatment of RTX-resistant disease.

Table 2
Characterization of RTX-(P-EPI)x and control conjugates.

No.	Conjugate	Polymer-precursor	P/Ab ratio	EPI/antibody (DAR)
1	RTX-EPI	–	–	3.1
2	RTX-(P-EPI)$_{3.1}$	ST-P-EPI-1	3.1	20.6
3	RTX-(P-EPI)$_{4.4}$	ST-P-EPI-2	4.4	20.7
4	RTX-(P-EPI)$_{5.6}$	ST-P-EPI-2	5.6	26.3
5	RTX-(P-EPI)$_{6.5}$	ST-P-EPI-1	6.5	42.9
6	IgG-(P-EPI)$_{3.6}$	ST-P-EPI-2	3.6	16.9

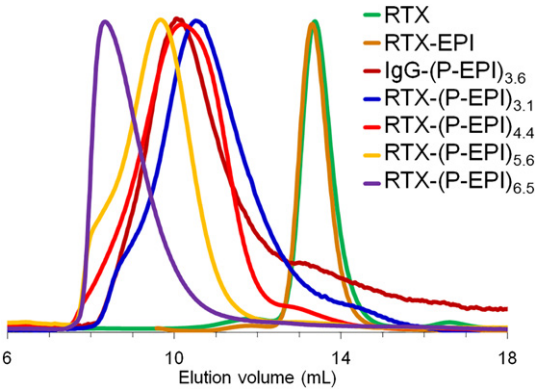

Fig. 2. SEC analysis of antibody-drug conjugates with different substitution.

3.4. Internalization of antibody-polymer-drug conjugate

CD20 is a non- or slowly internalizing antigen that remains on the cell surface when bound to a complementary antibody, i.e. RTX (Press et al., 1989; Law et al., 2004). To examine whether conjugation of P-EPI to RTX will enhance the internalization of RTX-P-EPI, Ramos cells were incubated in RTX-P-EPI with over-saturating level at 4 °C for 30 min. Cells were washed at 4 °C, and then kept at both 37 °C and 4 °C (in the presence of NaN_3), permissive and nonpermissive (+inhibitor) temperature for endocytosis, respectively. At 0, 30 min, 1, 2, and 3 h, cells were stained with Alexa Fluor-488 goat anti-human IgG secondary antibody. Flow cytometry was used to analyze the remaining surface RTX-P-EPI. Fig. 6A shows no detectable change over the 3 h course for the Ramos cells that kept at 4 °C. In contrast, surface levels of RTX-P-EPI decreased significantly when the cells were kept at 37 °C. Within 3 h, about 40% of RTX-P-EPI was lost from the cell surface,

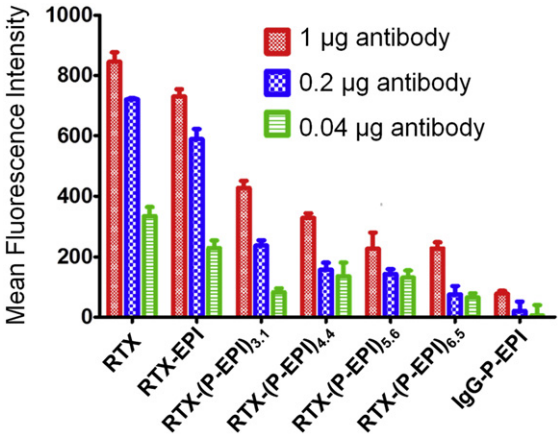

Fig. 3. The mean fluorescence intensity of Ramos cells following exposure to different amounts of RTX alone or antibody-drug conjugates. 2×10^5 Ramos cells in 50 μl medium was mixed with different samples (1, 0.2 or 0.04 μg in 20 μl PBS) and incubated at 4 °C for 30 min. The mixture was washed by medium twice to remove unbound sample. 100 μl secondary antibody (GAH-488, 1:200 diluted) was added and incubated at 4 °C for 30 min. After washing by PBS, the cells were analyzed by flow cytometry. All data are presented as mean ± SD (n = 3).

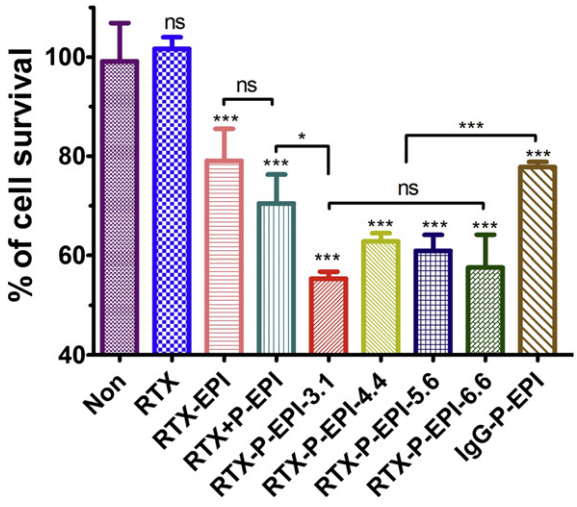

Fig. 4. In vitro cytotoxicity of RTX-P-EPI toward Ramos cells. RTX, RTX-EPI, RTX + P-EPI and IgG-P-EPI were used as references. 10^4 Ramos cells were seeded in each well of 96-well plates in 200 μl RPMI-1640 medium containing 10% FBS. Different samples (0.3 mg/ml × 15 μl) were added and incubated at 37 °C in a humidified atmosphere of 5% CO_2 (v/v). After 48 h, the number of viable cells was estimated using CCK-8 kit at 450 nm (630 nm as reference). One-way analysis of variance (ANOVA) coupled with Tukey's post hoc analysis was used to compare three or more groups (with p value <0.05 indicating statistically significant difference, * < 0.05, *** < 0.0001).

suggesting the conjugate RTX-P-EPI was internalized by the cells. This observation is coincident with a previous report by Law et al. that conjugation of monomethyl auristatin E (MMAE) to RTX resulted in internalization of RTX-vcMMAE (Law et al., 2004). Furthermore, confocal microscopy images (Fig. 6B) confirmed the internalization of RTX-P-EPI. After incubation at 37 °C for 3 h, fluorescence signals were detected not only on the surface (like RTX-Cy5), but also in the cytoplasm of Ramos cells, which indicated that RTX-P-EPI was internalized by the cells.

3.5. In vivo anti-tumor efficacy of RTX-P-EPI

The therapeutic potential of RTX-P-EPI was evaluated in male NOD SCID mice bearing human lymphoma xenografts. NOD SCID mice were subcutaneously implanted with Ramos cells (5×10^6 cells/200 μl saline) into the right flank. When tumors reached 100–200 mm^3, mice were treated intravenously with 20 mg/kg of RTX or RTX-equivalent dose of RTX-P-EPI (that dose led to an EPI dose of 1.5 mg/kg). Saline was injected as control. For comparison, RTX-EPI, RTX + EPI, RTX + P-EPI and IgG-P-EPI were also administered. Mice were treated with 4 doses at 3-day intervals. There are no significant differences until day 21 among various treatment groups except RTX-P-EPI vs. saline (the post hoc test p value is smaller than 0.05). However, RTX alone, RTX-EPI and the non-specific conjugate IgG-P-EPI only showed marginal effect. Mice treated with these regimens were soon killed due to rapid tumor development. By day 30, significant differences were found in the remaining three treatments. The p value of ANOVA is 0.0116, and both of the post hoc test p values of RTX-P-EPI vs. RTX + P-EPI and vs. RTX + EPI are <0.05 (Fig. 7).

The targeting effect was clearly demonstrated by comparison of RTX-P-EPI with a non-specific conjugate IgG-P-EPI, as both conjugates have similar Mw, thus the enhanced permeability and retention (EPR) effect could be ruled out. Importantly, by comparing RTX-P-EPI with equivalent RTX + EPI and RTX + P-EPI, the conjugate RTX-P-EPI demonstrated structural synergistic effect.

These results convincingly demonstrated that RTX-P-EPI is more effective in vivo than RTX-EPI, an ADC with a traditional design. In addition, body weight of the mice was closely recorded during and after treatment. The body weight loss of the mice treated with RTX-P-EPI was within acceptable limits and remained stable after withdrawal; there was no observed evidence of increased toxicity of RTX-P-EPI compared to controls (Supporting information Fig. S3).

3.6. Pharmacokinetics and biodistribution of ^{125}I labeled antibody-polymer-drug conjugates

The pharmacokinetic properties of ^{125}I labeled RTX, RTX-P-EPI and IgG-P-EPI were evaluated in male NOD SCID mice. Antibody was radiolabeled by ^{125}I and i.v. injected at 3.5 mg/kg (based on antibody for RTX, RTX-P-EPI, and IgG-P-EPI) single dose. The blood radioactivity time profiles of ^{125}I-labeled RTX-P-EPI and of RTX demonstrate the following: a) conjugation of over 20 epirubicin molecules (via multiple linear polymer carriers) to RTX did not accelerate its clearance; b) reduction of RTX for conjugation of polymer-precursor did not destabilize the RTX structure via binding to critical disulfide bonds when

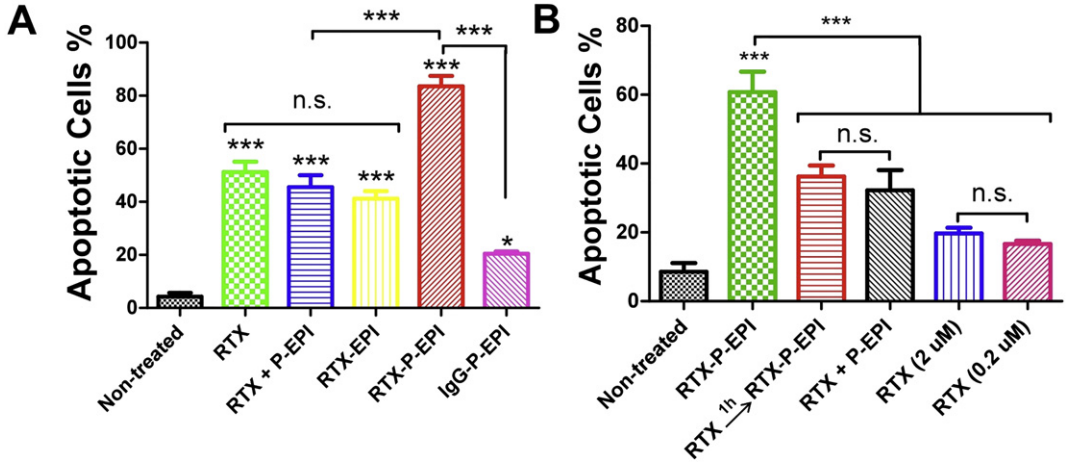

Fig. 5. In vitro cytotoxicities of conjugates toward (A) Ramos cells and (B) Raji cells. Apoptosis induction in Ramos and Raji cells was analyzed by Annexin V/PI binding assay. Incubation time was 48 h for Ramos cells and 24 h for Raji cells. The following indications apply to the figure. *Non-treated*, cells in culture medium; *RTX*, rituximab (0.2 μM); *RTX + P-EPI*, mixture of rituximab and P-EPI (0.2 μM based on rituximab, the concentration of P-EPI was equal to the content of RTX-P-EPI); *RTX-EPI*, rituximab-EPI conjugate (0.2 μM based on rituximab); *RTX* $\xrightarrow{1h}$ *RTX-P-EPI*, cells were preblocked by rituximab (2 μM), followed (1 h later) by RTX-P-EPI conjugate (0.2 μM); *RTX-P-EPI*, RTX-P-EPI conjugate (0.2 μM based on rituximab); *IgG-P-EPI*, IgG-P-EPI conjugate (0.2 μM based on IgG). Percentage of apoptotic cells was quantified by flow cytometry. All data are presented as mean ± SD (n = 3). Statistical analysis was performed by one-way analysis of variance (ANOVA) coupled with Tukey's post hoc analysis to compare three or more groups (with p value <0.05 indicating statistically significant difference; * < 0.05, *** < 0.0001, n.s.: no significant difference).

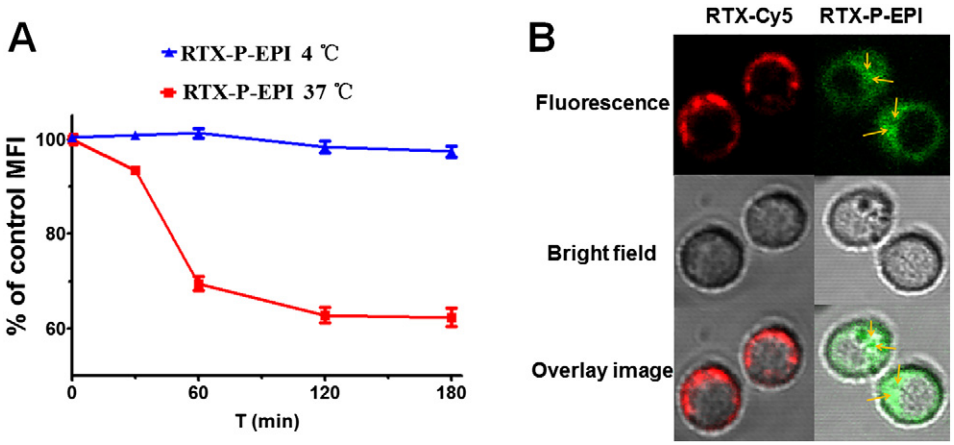

Fig. 6. Internalization of antibody-polymer-drug conjugate into Ramos cells. Flow cytometry (A) and confocal microscopy (B) analysis.

exposed to sheer stress in vivo (Fig. 8). These results strongly suggest that our ADC design will not compromise the pharmacokinetic properties of the antibody (see Supplementary information Table S1 for PK parameters).

We also compared biodistribution of RTX, RTX-P-EPI and IgG-P-EPI labeled by ^{125}I in male NOD SCID mice bearing s.c. xenograft tumor model. At 72 h after intravenous injection, tumor uptake of ^{125}I-RTX-P-EPI was higher than that in major organs except spleen. Particularly, the level of targeted antibody-polymer-drug conjugate in the tumor (^{125}I-RTX-P-EPI, 0.75% ID/g tissue), which was comparable to that of RTX (0.71% ID/g tissue), was 3-fold higher than the non-targeted conjugate (^{125}I-IgG-P-EPI, 0.25% ID/g tissue) (Fig. 9). These results suggest that although attachment of polymer-drug precursors to RTX results in partial loss of binding affinity, long-circulation property of RTX-P-EPI enables to achieve comparable tumor uptake as RTX in our model.

4. Discussion

From the structure-function point of view, antibody–drug conjugates belong to the "targeted chemotherapeutics" category of anti-cancer drugs. Historically, antibody and/or antibody Fab' fragment have been incorporated into water-soluble polymer-anticancer drug conjugates as targeting moieties to improve the therapeutic outcome and to reduce the toxicity of anticancer agents (Říhová and Kopeček, 1985; Říhová et al., 1988, 2002; Pimm et al., 1993; Omelyanenko et al., 1996; Hongrapipat et al., 2008; Lu et al., 1999, 2003; Shiah et al., 2001; Jelínková et al., 1998; KováŘ et al., 2002; Chytil et al., 2010; Pola et al., 2013). For example, a comparison of the efficacy between non-targeted and OV-TL16 mAb fragment-targeted HPMA copolymer-mesochlorin e_6 conjugates (P-Mce$_6$ vs. P-Fab'-Mce$_6$) for treatment of OVCAR-3 xenografts in nude mice has been performed. Results clearly indicate the advantage of targeted treatment (Lu et al., 1999, 2003). Omelyanenko et al. (1996) performed detailed studies to investigate the impact of conjugation chemistry on binding affinity of modified antibody conjugates. Differences in Ka (affinity constant) suggested random modification of lysine residues via amide bond lead to conjugate heterogeneity and impaired antigen binding; site-specific modification results in superior property. However, unlike classic ADCs in which monoclonal antibody itself can induce cancer cell death, an antibody (or antibody fragment) in the aforementioned early studies served as targeting moiety, and did not have therapeutic function.

Despite a growing number of ADCs currently in clinical trials or preclinical development, there still remains space to explore new approaches for the treatment of hematologic malignancies. For example, a new therapy that combines high efficacy with enhanced tolerability is needed. Efficacy and safety are two major issues. Due to limited attachment sites, in current ADCs, more and more potent toxins (IC_{50} from nmol to pmol) are being investigated to achieve DAR 2 (2 toxins conjugated to one mAb). Such strategy raises toxicity concerns. It was reported recently that six patients with acute myeloid leukemia (AML) have been identified with liver

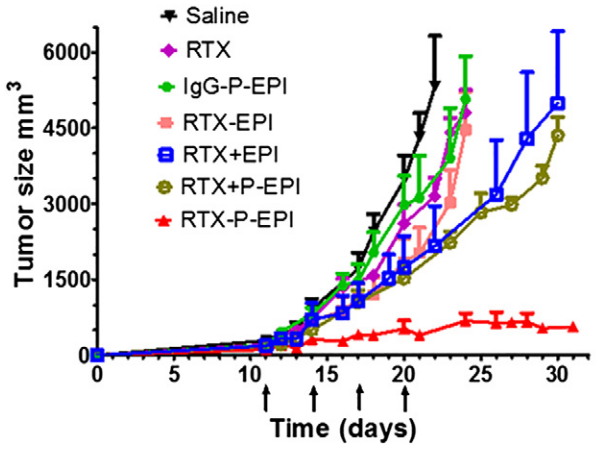

Therapeutics	Dose (mg/kg)	
	RTX	EPI
RTX	20	-
RTX-P-EPI	**20**	**1.5**
RTX+P-EPI	20	1.5
RTX+EPI	20	1.5
RTX-EPI	20	0.22
IgG-P-EPI	23[a]	1.5

[a] *IgG dose.*

Fig. 7. Antitumor activity of RTX-P-EPI in B-cell lymphoma model. NOD SCID male mice were inoculated with 5×10^6 Ramos cells into the right flank. Treatment was initiated when the mean tumor size reached 100 mm^3 or above. Four doses with 20 mg/kg of RTX (1.5 mg/kg equivalent EPI in 20 mg/kg RTX-P-EPI) on days 11, 14, 17, and 20 (arrows) were administered via tail vein. Saline was used as non-treated control. RTX, RTX-EPI, mixture of RTX + P-EPI, mixture of RTX + EPI and IgG-P-EPI were also evaluated. The data are presented as mean ± SD (n = 4–5).

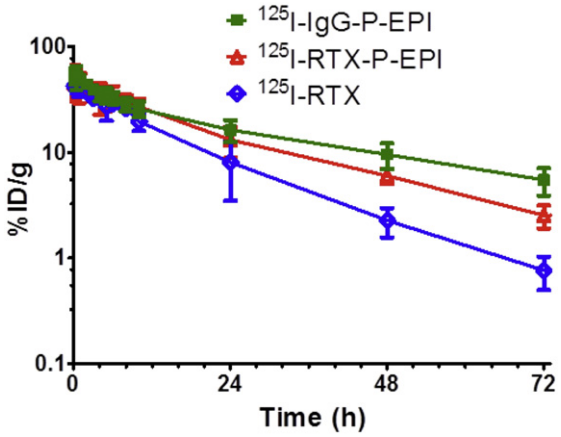

Fig. 8. Pharmacokinetic profiles of ^{125}I-labeled conjugates IgG-P-EPI, RTX and RTX-P-EPI in male NOD SCID mice. Data obtained using the radioactivity count method was plotted as percentage of injected dose per gram of tissue (% ID/g). All data are expressed as mean ± standard deviation (n = 3).

toxicities in clinical trials and four of them have died (http://mobile.reuters.com/article/idUSKBN14G13V).

Semitelechelic (ST) polymers are linear macromolecules having a reactive functional group at one end of the polymer chain (Kamei and Kopeček, 1995). The single functional group provided the opportunity to conjugate or graft the macromolecule to other species or surfaces (Lu et al., 1998). ST-HPMA copolymers have been used in the synthesis of star copolymers, e.g., by attachment to amino groups of dendrimers (Wang et al., 2000) or for modification of antibodies. The chemistries used for the antibody modification varied. The synthesis of antibody polymer conjugates by reaction with polymer precursors containing several attachment points, results in partially crosslinked conjugates containing antibody molecules and several polymer chains (Říhová and Kopeček, 1985; Tappertzhofen et al., 2013; Kovář et al., 2002). The use of ST-copolymers results in well-defined *star*-like conjugates where one antibody molecule is decorated with several polymer chains (Kovář et al., 2002; Etrych et al., 2009; Tappertzhofen et al., 2014; Lidický et al., 2015). The attachment of polymer chains is performed either non-specifically by reaction of ST polymers with accessible amino groups of lysine (Kovář et al., 2002) or more specifically by reduction of the antibody disulfide bonds and attachment of ST copolymer via thiol-ene reaction (Etrych et al., 2009; Lidický et al., 2015). Alternatively, the amino groups of lysine may be modified (non-specifically) by 2-iminothiolane and the ST polymer attached via thiol-ene reaction (Etrych et al., 2007, 2009).

In this study, we present a new generation antibody-drug conjugates (ADCs) that integrated two traditional approaches (antibody targeting and polymer therapeutics) into one 'hybrid' product with the potential to not only enhance treatment efficacy but also improve tolerability for patients with B-cell lymphomas. A conventional cytotoxic agent epirubicin was incorporated onto HPMA polymer carrier by a controlled living polymerization technique, resulting in a well-defined semitelechelic maleimide functionalized polymer-drug conjugate. This precursor was attached to RTX, a chimeric anti-CD20 mAb, to generate a new type of ADC, RTX-P-EPI. It is based on our long-term experience with HPMA copolymer-drug conjugates (Yang and Kopeček, 2016), and the advances in the field of antiCD20 therapeutics (Chu and Polson, 2013; Law et al., 2004). Previously, RTX has been conjugated with both free drug doxorubicin (DOX) (Braslawsky et al., 1991), liposomal Dox (Sapra and Allen, 2002), and HPMA copolymer-DOX conjugates (Lidický et al., 2015). Unfortunately, these antibody-drug conjugates were found to be therapeutically ineffective. Initially, the failure was explained by the CD20 non-internalization property. However, Law et al. (2004) evaluated a RTX-based ADC using MMAE, whose IC_{50} is 50–200 folds lower than that of DOX. Interestingly, internalization of the conjugate was demonstrated and the antitumor efficacy of the conjugate (RTX-vcMMAE) in xenograft model of CD20-positive lymphoma was proved. Internalization of iron oxide nanoparticles targeted with CD20+ single chain variable fragment antibody-streptavidin fusion protein in the MC126 B lymphoma cell line was also observed (Wang et al., 2013). Similarly, the internalization and antitumor efficacy of our conjugate, RTX-P-EPI, was established.

One of the barriers for RTX clinical application is the resistance. Rituximab resistance pathways remain uncertain. One of the key factors for resistance development is frequently repeated relatively high doses. The mechanistic factors involved are the altered signaling, resulting in the overexpression of anti-apoptotic proteins of the Bcl-2 family and leading to resistance to apoptosis. Interestingly, by comparing with the mixture of RTX and polymer-drug conjugate (P-EPI), RTX-P-EPI showed 1.5 times higher in vitro cytotoxicity and significantly delayed tumor growth. This higher in vitro cytotoxicity and in vivo antitumor efficacy indicated synergistic effect. EPI is reported to up-regulate Bax and Bak (the pro-apoptotic Bcl-2 family proteins); this may re-sensitize resistant cells to rituximab-mediated apoptosis. Therefore, the results suggest that this new design possesses synergistic potential of immunotherapy combined with established macromolecular therapy. Moreover, a conventional chemo-agent could be utilized to generate

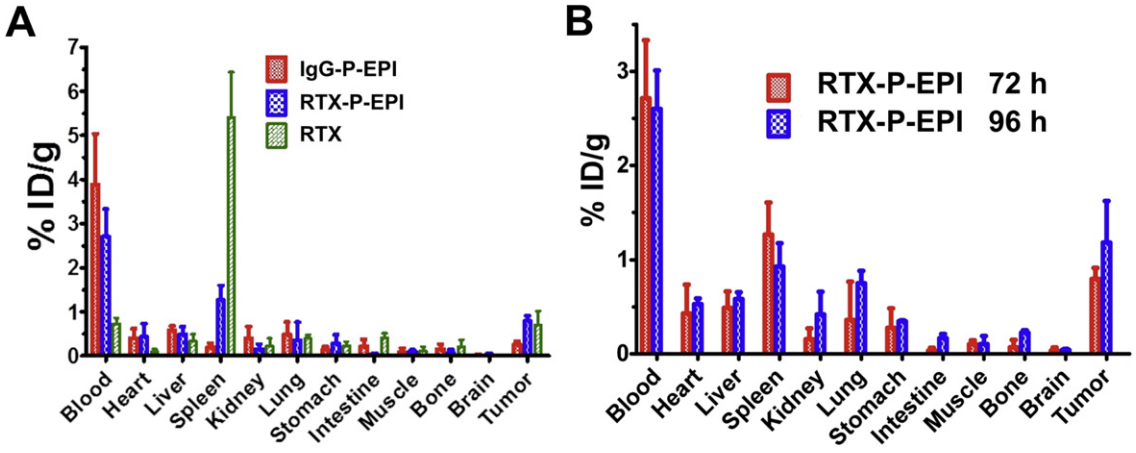

Fig. 9. Biodistribution of ^{125}I-labeled RTX, RTX-P-EPI, and non-specific IgG-P-EPI in Ramos lymphoma-bearing NOD SCID mice at 72 h after intravenous administration. Data obtained using the radioactivity count method was plotted as percentage of injected dose per gram of tissue (% ID/g). All data are expressed as mean ± standard deviation (n = 3).

highly effective ADCs and concomitantly reduce the risk of off-target toxicity.

Conflict of interest

The authors are co-inventors on a provisional patent application related to this work assigned to the University of Utah.

Funding

The research was supported in part by the University of Utah Project 00053 (JK) and SEED Grant 51900204 (JY).

Acknowledgements

We would like to thank Dr. P. Shami for valuable discussions, and Chieh-Hsiang Yang from Dr. Janát-Amsbury laboratory for his support in animal study.

Appendix A. Supplementary data

Supplementary data to this article can be found online at http://dx.doi.org/10.1016/j.ejps.2017.02.034.

References

Alley, S.C., Okeley, N.M., Senter, P.D., 2010. Antibody–drug conjugates: targeted drug delivery for cancer. Curr. Opin. Chem. Biol. 14 (4), 529–537.

Braslawsky, G.R., Kadow, K., Knipe, J., McGoff, K., Edson, M., Kaneko, T., Greenfield, R.S., 1991. Adriamycin (hydrazone)-antibody conjugates require internalization and intracellular acid hydrolysis for antitumor activity. Cancer Immunol. Immunother. 33, 367–374.

Casi, G., Neri, D., 2012. Antibody-drug conjugates: basic concepts, examples and future perspectives. J. Control. Release 161, 422–428.

Chari, R.V., Miller, M.L., Widdison, W.C., 2014. Antibody-drug conjugates: an emerging concept in cancer therapy. Angew. Chem. Int. Ed. 53, 3796–3827.

Cheson, B.D., Leonard, J.P., 2008. Monoclonal antibody therapy for B-cell non-Hodgkin's lymphoma. N. Engl. J. Med. 359, 613–626.

Chu, T.-W., Kopeček, J., 2015. Drug-free macromolecular therapeutics – a new paradigm in polymeric nanomedicines. Biomater. Sci. 3, 908–922.

Chu, Y.W., Polson, A., 2013. Antibody-drug conjugates for the treatment of B-cell non-Hodgkin's lymphoma and leukemia. Future Oncol. 9, 355–368.

Chytil, P., Etrych, T., Kříž, J., Šubr, V., Ulbrich, K., 2010. *N*-(2-hydroxypropyl)methacrylamide-based polymer conjugates with pH-controlled activation of doxorubicin for cell-specific or passive tumour targeting. Synthesis by RAFT polymerisation and physicochemical characterisation. J. Control. Release 41, 473–482.

Ducry, L., Stump, B., 2010. Antibody-drug conjugates: linking cytotoxic payloads to monoclonal antibodies. Bioconjug. Chem. 21, 5–13.

Etrych, T., Mrkvan, T., Říhová, B., Ulbrich, K., 2007. Star-shaped immunoglobulin-containing HPMA-based conjugates with doxorubicin for cancer therapy. J. Control. Release 122, 31–38.

Etrych, T., Strohalm, J., Kovář, L., Kabešová, M., Říhová, B., Ulbrich, K., 2009. HPMA copolymer conjugates with reduced anti-CD20 antibody for cell-specific drug targeting. I. Synthesis and in vitro evaluation of binding efficacy and cytostatic activity. J. Control. Release 140, 18–26.

Gergel, D., Cederbaum, A.-I., 1996. Inhibition of the catalytic activity of alcohol dehydrogenase by nitric oxide is associated with S nitrosylation and the release of zinc. Biochemistry 35, 16186–16194.

Hongrapipat, J., Kopečková, P., Liu, J., Prakongpan, S., Kopeček, J., 2008. Combination chemotherapy and photodynamic therapy with Fab' fragment targeted HPMA copolymer conjugates in human ovarian carcinoma cells. Mol. Pharm. 5, 696–709.

Jagadeesh, D., Smith, M.R., 2016. Antibody drug conjugates (ADCs): changing the treatment landscape of lymphoma. Curr. Treat. Options in Oncol. 17:55. http://dx.doi.org/10.1007/s11864-016-0428-y.

Jelínková, M., Strohalm, J., Plocová, D., Šubr, V., Šťastný, M., Ulbrich, K., Říhová, B., 1998. Targeting of human and mouse T-lymphocytes by monoclonal antibody-HPMA copolymer-doxorubicin conjugates directed against different T-cell surface antigens. J. Control. Release 52, 253–270.

Kamei, S., Kopeček, J., 1995. Prolonged blood circulation in rats of nanospheres surface-modified with semitelechelic poly[*N*-(2-hydroxypropyl)methacrylamide]. Pharm. Res. 12, 663–668.

Kopeček, J., Bažilová, H., 1973. Poly[*N*-(2-hydroxypropyl)methacrylamide]. 1. Radical polymerization and copolymerization. Eur. Polym. J. 9, 7–14.

Kovář, M., Strohalm, J., Etrych, T., Ulbrich, K., Říhová, B., 2002. Star structure of antibody-targeted HPMA copolymer-bound doxorubicin: a novel type of polymeric conjugate for targeted drug delivery with potent antitumor effect. Bioconjug. Chem. 13, 206–215.

Law, C.-L., Cerveny, C.G., Gordon, K.A., Klussman, K., Mixan, B.J., Chace, D.F., Meyer, D.L., Doronina, S.O., Siegall, C.B., Francisco, J.A., Senter, P.D., Wahl, A.F., 2004. Efficient elimination of B-lineage lymphomas by anti-CD20 – auristatin conjugates. Clin. Cancer Res. 10, 7842–7851.

Leget, G.A., Czuczman, M.S., 1998. Use of rituximab, the new FDA-approved antibody. Curr. Opin. Oncol. 10, 548–551.

Lidický, O., Janoušková, O., Strohalm, J., Alam, M., Klener, P., Etrych, T., 2015. Anti-lymphoma efficacy comparison of anti-CD20 monoclonal antibody-targeted and non-targeted star-shaped polymer-prodrug conjugates. Molecules 20, 19849–19864.

Liu, J., Kopečková, P., Bühler, P., Wolf, P., Pan, H., Bauer, H., Elsässer-Beile, U., Kopeček, J., 2009. Biorecognition and subcellular trafficking of HPMA copolymer – anti-PSMA antibody conjugates by prostate cancer cells. Mol. Pharm. 6, 959–970.

Lu, Z.-R., Kopečková, P., Wu, Z., Kopeček, J., 1998. Functionalized semitelechelic poly[*N*-(2-hydroxypropyl)methacrylamide] for protein modification. Bioconjug. Chem. 9, 793–804.

Lu, Z.-R., Kopečková, P., Kopeček, J., 1999. Polymerizable Fab' antibody fragments for targeting of anticancer drugs. Nat. Biotechnol. 17, 1101–1104.

Lu, Z.-R., Shiah, J.-G., Kopečková, P., Kopeček, J., 2003. Polymerizable Fab' antibody fragment targeted photodynamic cancer therapy in nude mice. STP Pharma Sci. 13, 69–75.

Mehta, A., Forero-Torres, A., 2015. Development and integration of antibody-drug conjugate in non-Hodgkin lymphoma. Curr. Oncol. Rep. 17 (9):41. http://dx.doi.org/10.1007/s11912-015-0466-9.

Mitsukami, Y., Donovan, M.S., Lowe, A.B., McCormick, C.L., 2001. Water-soluble polymers. 81. Direct synthesis of hydrophilic styrenic-based homopolymers and block copolymers in aqueous solution via RAFT. Macromolecules 34, 2248–2256.

Omelyanenko, V., Kopečková, P., Gentry, C., Shiah, J.-G., Kopeček, J., 1996. HPMA copolymer – anticancer drug – OV-TL16 antibody conjugates. 1. Influence of the method of synthesis on the binding affinity to OVCAR-3 ovarian carcinoma cells in vitro. J. Drug Target. 3, 357–373.

Pimm, M.V., Perkins, A.C., Duncan, R., Ulbrich, K., 1993. Targeting of *N*-(2 hydroxypropyl)methacrylamide copolymer-doxorubicin conjugate to the hepatocyte galactose receptor in mice: visualisation and quantification by gamma scintigraphy as a basis for clinical targeting studies. J. Drug Target. 1, 125–131.

Pola, R., Laga, R., Ulbrich, K., Sieglová, I., Král, V., Fábry, M., Kabešová, M., Kovář, M., Pechar, M., 2013. Polymer therapeutics with a coiled coil motif targeted against murine BCL1 leukemia. Biomacromolecules 14, 881–889.

Press, O.W., Farr, A.G., Borroz, K.I., Anderson, S.K., Martin, P.J., 1989. Endocytosis and degradation of monoclonal antibodies targeting human B-cell malignancies. Cancer Res. 49, 4906–4912.

Richter, M., Yumul, R., Saydaminova, K., Wang, H., Gough, M., Baldessari, A., Cattaneo, R., Lee, F., Wang, C.H., Jang, H., Astier, A., Gopal, A., Carter, D., Lieber, A., 2016. Preclinical safety, pharmacokinetics, pharmacodynamics, and biodistribution studies with Ad35K++ protein: a novel rituximab cotherapeutic. Mol. Ther. Methods Clin. Dev. 5, 16013.

Říhová, B., Kopeček, J., 1985. Biological properties of targetable poly[*N*-(2-hydroxypropyl)methacrylamide] – antibody conjugates. J. Control. Release 2, 289–310.

Říhová, B., Kopečková, P., Strohalm, J., Rossmann, P., Větvička, V., Kopeček, J., 1988. Antibody directed affinity therapy applied to the immune system: *in vivo* effectiveness and limited toxicity of daunomycin conjugates to HPMA copolymers and targeting antibody. Clin. Immunol. Immunopathol. 46, 100–114.

Říhová, B., Strohalm, J., Kubáčková, K., Jelínková, M., Hovorka, O., Kovář, M., Plocová, D., Šírová, M., Šťastný, M., Rozprimová, L., Ulbrich, K., 2002. Acquired and specific immunological mechanisms co-responsible for efficacy of polymer-bound drugs. J. Control. Release 78, 97–114.

Sapra, P., Allen, T.M., 2002. Internalizing antibodies are necessary for improved therapeutic efficacy of antibody targeted liposomal drugs. Cancer Res. 62, 7190–7194.

Seyfizadeh, N., Seyfizadeh, N., Hasenkamp, J., Huerta-Yepez, S., 2016. A molecular perspective on rituximab: a monoclonal antibody for B cell non-Hodgkin lymphoma and other affections. Crit. Rev. Oncol. Hematol. 97, 275–290.

Shiah, J.-G., Sun, Y., Kopečková, P., Peterson, C.M., Straight, R.C., Kopeček, J., 2001. Combination chemotherapy and photodynamic therapy of targetable *N*-(2-hydroxypropyl)methacrylamide copolymer – doxorubicin/mesochlorin e_6 - OV-TL16 antibody immunoconjugates. J. Control. Release 74, 249–253.

Siegel, R., Miller, K.D., Jemal, A., 2016. Cancer statistics, 2016. CA Cancer J. Clin. 66, 7–30.

Tao, L., Liu, J., Xu, J., Davis, T.P., 2009. Synthesis and bioactivity of poly(HPMA)-lysozyme conjugates: the use of novel thiazolidine-2-thione coupling chemistry. Org. Biomol. Chem. 7, 3481–3485.

Tappertzhofen, K., Metz, V.V., Hubo, M., Barz, M., Postina, R., Jonuleft, H., Zentel, R., 2013. Synthesis of maleimide-functionalized HPMA copolymers and in vitro characterization of the aRAGE- and human immunoglobulin (huIgG)-polymer conjugates. Macromol. Biosci. 13, 203–214.

Tappertzhofen, K., Bednarczyk, M., Koynov, K., Bros, M., Grabbe, S., Zentel, R., 2014. Toward anticancer immunotherapeutics: well-defined polymer-antibody conjugates for selective dendritic cell targeting. Macromol. Biosci. 14, 1444–1457.

Tolcher, A.W., Sugarman, S., Gelmon, K.A., 1999. Randoomized phase II study of BR96-doxorubicin conjugate in patients with metastatic breast cancer. J. Clin. Oncol. 17, 478–484.

Ulbrich, K., Šubr, V., Strohalm, J., Plocová, D., Jelínková, M., Říhová, B., 2000. Polymeric drugs based on conjugates of synthetic and natural macromolecules. I. Synthesis and physico-chemical characterisation. J. Control. Release 64, 63–79.

Wang, D., Kopečková, P., Minko, T., Nanayakkara, V., Kopeček, J., 2000. Synthesis of star-like *N*-(2-hydroxypropyl)methacrylamide copolymers – potential drug carriers. Biomacromolecules 1, 313–319.

Wang, T., Kievit, F.M., Veiseh, O., Arami, H., Stephen, Z.R., Fang, C., Liu, Y., Ellenbogen, R.G., Zhang, M., 2013. Targeted cell uptake of noninternalizing antibody through conjugation to iron oxide nanoparticles in primary central nervous system lymphoma. World Neurosurg. 80, 134–141.

Wu, A.M., Senter, P.D., 2005. Arming antibodies: prospects and challenges for immunoconjugates. Nat. Biotechnol. 23, 1137–1146.

Yang, J., Kopeček, J., 2016. Design of smart HPMA copolymer-based nanomedicines. J. Control. Release 240, 9–23.

Yang, J., Zhang, R., Radford, D.C., Kopeček, J., 2015. FRET-trackable biodegradable HPMA copolymer-epirubicin conjugates for ovarian carcinoma therapy. J. Control. Release 218, 36–44.

Zelenetz, A.D., Gordon, L.I., Wierda, W.G., Abramson, J.S., Advani, R.H., Andreadis, C.B., Bartlett, N., Byrd, J.C., Czuczman, M.S., Fayad, L.E., Fisher, R.I., Glenn, M.J., Harris, N.L., Hoppe, R.T., Horwitz, S.M., Kelsey, C.R., Kim, Y.H., Krivacic, S., LaCasce, A.S., Nademanee, A., Porcu, P., Press, O., Rabinovitch, R., Reddy, N., Reid, E., Saad, A.A., Sokol, L., Swinnen, L.J., Tsien, C., Vose, J.M., Yahalom, J., Zafar, N., Dwyer, M., Sundar, H., 2014. Non-Hodgkin's lymphomas, version 4.2014. Natl. Compr. Cancer Netw. 12, 1282–1303.

Zhang, L.-B., Zhao, W.-G., Liu, X.-Y., Wang, G.-L., Wang, Y., Li, D., Xie, L.-Z., Gao, Y., Deng, H.-T., Gao, W.-P., 2015. Site-selective in situ growth of fluorescent polymer-antibody conjugates with enhanced antigen detection by signal amplification. Biomaterials 64, 2–9.